

Supplementary Material Cover Sheet

Effects of divalent metal cations and inorganic anions on the transport of tetracycline in saturated porous media: Column experiments and numerical simulations

Wenwen Li ^{1, a}, Haojing Zhang ^{1, a}, Taotao Lu ^{2, 3}, Yanxiang Li ⁴, Yumeng Song ¹,
Zhongbo Shang ¹, Shanhu Liu ¹, Deliang Li ¹, and Zhichong Qi ^{1, 2, *}

¹ Henan Joint International Research Laboratory of Environmental Pollution Control Materials, College of Chemistry and Chemical Engineering, Henan University, Kaifeng 475004, China

² Ministry of Education Key Laboratory of Pollution Processes and Environmental Criteria, Nankai University, Tianjin 300350, China

³ Department of Hydrology, University of Bayreuth, Bayreuth D-95440, Germany

⁴ The Testing Center of Shandong Bureau of China Metallurgical Geology Bureau, Jinan 250014, China

Manuscript prepared for *Environmental Science: Processes & Impacts*

*Corresponding author: Zhichong Qi (qizhichong1984@163.com);

^a Wenwen Li and Haojing Zhang contributed equally.

Number of pages: 17

Number of tables: 6

Number of figures: 7

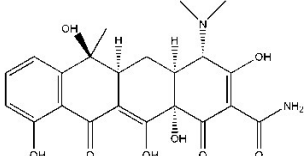
S1. Adsorption of inorganic anions onto sand

Adsorption studies were conducted to determine the adsorption capacity of inorganic anions onto sand under different solution chemistry conditions. First, approximately 3 g quartz sand and 20 mL of inorganic anion solutions (different concentrations, see Table 2) were added to each of a series of 20-ml amber glass vials. Then, the vials were equilibrated for 12 h by horizontally shaking (the duration equal to the transport experiment). Then, the vials were centrifuged at 5000 rpm for 20 min and the supernatants were withdrawn. The concentrations of anionic species which could be analyzed were quantified by ion chromatography (IC) with a system from ThermoFisher (Dionex ICS-2100, Dionex IonPac® AS15 column). The adsorbed inorganic anions were then determined by the difference between the initial and final inorganic anion concentrations in the aqueous phase. All experiments were run in triplicate. The test results are presented in Table S3.

S2. Procedures used to obtain the retention profiles of tetracycline in the column

To obtain the retention profiles of tetracycline in the column at the end of the transport experiments, the sand columns were dissected into 10 layers of 1-cm segments and subsequently re-entrained to extraction solutions (methanol), then vibrated on a horizontal motion shaker for 24 h at the ambient temperature.^{S1} Then the vials were centrifuged at 3,500 rpm for 20 min, and the supernatants were withdrawn to measure the concentrations of tetracycline. The sand segments were oven-dried at 90 °C overnight to obtain the dry weight of the sand in each segment.

Table S1. Selected properties of tetracycline

Molecular formula	Chemical structure	Molecular weight (g/mol)	Solubility (g/L) ^a	Log K_{ow} ^b	pK_a ^b
$C_{22}H_{24}N_2O_8$		444.43	1.7	-1.37	$pK_{a1}=3.3$ $pK_{a2}=7.7$ $pK_{a3}=9.3$

^a Derived from Chang et al.^{S2}.

^b Derived from Li et al.^{S3}.

Table S2. ζ -potential of sand under different solution chemistry conditions

No.	Background solution ^a	pH	ζ -potential of sand (mV) ^a
1	DI water	5.0	-23.1 \pm 0.9
2	0.1 mM Mg(NO ₃) ₂	5.0	-20.3 \pm 0.5
3	0.1 mM Ca(NO ₃) ₂	5.0	-18.2 \pm 1.3
4	0.1 mM Pb(NO ₃) ₂	5.0	-16.2 \pm 0.7
5	0.1 mM Cu(NO ₃) ₂	5.0	-14.7 \pm 1.6
6	10 mM NaCl	5.0	-16.5 \pm 1.0
7	10 mM NaNO ₃	5.0	-17.2 \pm 1.5
8	10 mM Na ₂ SO ₄	5.0	-18.5 \pm 0.9
9	10 mM NaH ₂ PO ₄	5.0	-21.7 \pm 1.0
10	0.1 mM CaCl ₂	5.0	-18.9 \pm 0.5
11	0.2 mM CaSO ₄	5.0	-16.2 \pm 2.1
12	1.0 mM Ca(NO ₃) ₂	5.0	-12.6 \pm 0.3
13	1.0 mM CaCl ₂	5.0	-13.5 \pm 1.5
14	2.0 mM CaSO ₄	5.0	-11.8 \pm 0.6

^a Zeta potential of quartz sand; values after \pm sign represent standard deviation of five replicates.

Table S3. Adsorption amount of inorganic anions onto sand. Error bars represent standard deviations from replicate experiments (n=3)

No.	Background solution	pH	<i>q</i> (mg anions/kg-sand)
1	10 mM Cl ⁻	5.0	3.5 ± 0.8
2	10 mM NO ₃ ⁻	5.0	11.3 ± 1.5
3	10 mM SO ₄ ²⁻	5.0	20.4 ± 2.6
4	10 mM H ₂ PO ₄ ⁻	5.0	36.7 ± 1.9
5	0.2 mM Cl ⁻	5.0	1.3 ± 0.2
6	0.2 mM SO ₄ ²⁻	5.0	7.9 ± 0.9
7	2.0 mM Cl ⁻	5.0	4.1 ± 0.7
8	2.0 mM NO ₃ ⁻	5.0	8.8 ± 1.2
9	2.0 mM SO ₄ ²⁻	5.0	15.5 ± 2.3

Table S4. Mass balance expressed as percentage of effluent mass, eluted mass during each flushing step, and mass recovered from column

Column No.	Background solution	pH	Effluent Mass (%)	Eluted mass (%)	Mass recovered from column (%)	Mass balance ^a (%)
1	DI water	5.0	68.5	4.4	17.3	90.2
2	0.1 mM Mg(NO ₃) ₂	5.0	65.3	10.5	17.3	93.1
3	0.1 mM Ca(NO ₃) ₂	5.0	64.2	10.8	15.0	90.0
4	0.1 mM Pb(NO ₃) ₂	5.0	43.1	16.9	30.1	90.1
5	0.1 mM Cu(NO ₃) ₂	5.0	14.2	11.3	63.7	89.2
6	10 mM NaCl	5.0	74.6	5.9	12.6	93.1
7	10 mM NaNO ₃	5.0	79.2	5.9	12.2	97.3
8	10 mM Na ₂ SO ₄	5.0	82.3	6.3	9.4	98.0
9	10 mM NaH ₂ PO ₄	5.0	87.9	7.5	6.2	101
10	0.1 mM CaCl ₂	5.0	64.3	9.1	17.9	91.3
11	0.2 mM CaSO ₄	5.0	64.4	11.0	22.6	98.0
12	1.0 mM CaCl ₂	5.0	62.5	8.9	19.9	91.3
13	1.0 mM Ca(NO ₃) ₂	5.0	63.7	8.5	19.3	91.5
14	2.0 mM CaSO ₄	5.0	65.5	11.8	20.7	98.0

^a Mass balance was calculated as: (effluent mass + eluted mass + mass recovered from column)/mass injected.

Table S5. The amounts of tetracycline adsorption (q) onto sand in the presence of different inorganic anions (the mass of sand was 3 g)

No.	Background solution	pH	Initial concentration of tetracycline (mg.L ⁻¹)	q (mg tetracycline/kg-sand)
1	10 mM Cl ⁻	5.0	10	30.6 ± 0.5
2	10 mM NO ₃ ⁻	5.0	10	27.9 ± 0.4
3	10 mM SO ₄ ²⁻	5.0	10	24.2 ± 0.1
4	10 mM H ₂ PO ₄ ⁻	5.0	10	17.4 ± 0.6
5	0.2 mM Cl ⁻	5.0	10	35.9 ± 0.9
6	0.2 mM SO ₄ ²⁻	5.0	10	38.6 ± 0.6
7	2.0 mM Cl ⁻	5.0	10	39.3 ± 0.1
8	2.0 mM NO ₃ ⁻	5.0	10	40.1 ± 0.5
9	2.0 mM SO ₄ ²⁻	5.0	10	40.8 ± 0.6

Table S6. Properties of different anions

Parameter	Chloride	Nitrate	Sulfate	Phosphate
Molecular formula	Cl ⁻	NO ₃ ⁻	SO ₄ ²⁻	H ₂ PO ₄ ⁻
Molar mass (g mol ⁻¹)	35	62	96	97
Ionic radius (R _{ion}) (×10 ⁻¹⁰ m)	1.81 ^a	1.89 ^b	2.15 ^a	2.38 ^a
Hydrated radius (R _{hyd}) (×10 ⁻¹⁰ m)	3.80 ^a	3.35 ^b	3.00 ^a	3.02 ^a

^a Derived from Kiriukhin and Collins ^{S5}.

^b Derived from Tansel ^{S6}.

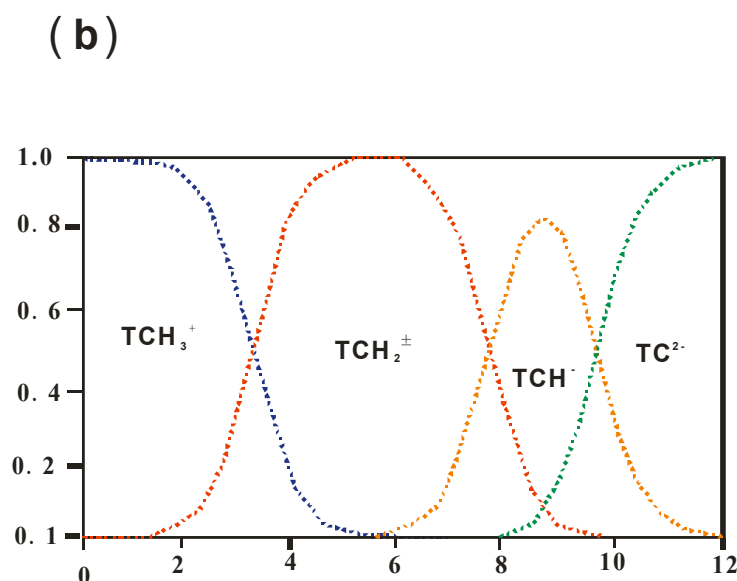
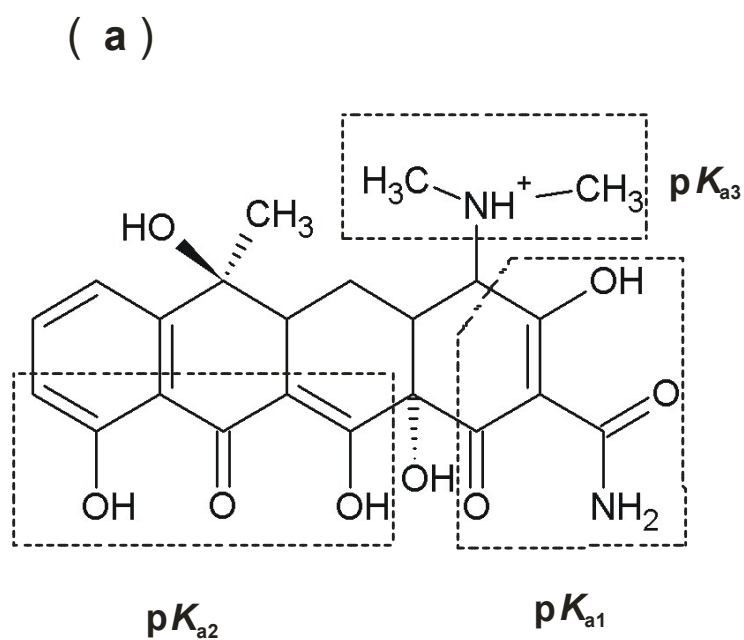


Fig S1. (a) Structure of tetracycline. The regions framed by dashed lines represent the three functional groups associated with the corresponding acidic dissociation constants (pK_a); and (b) pH-dependent speciation of the whole tetracycline molecular and the functional groups, respectively. TC is abbreviation of tetracycline.

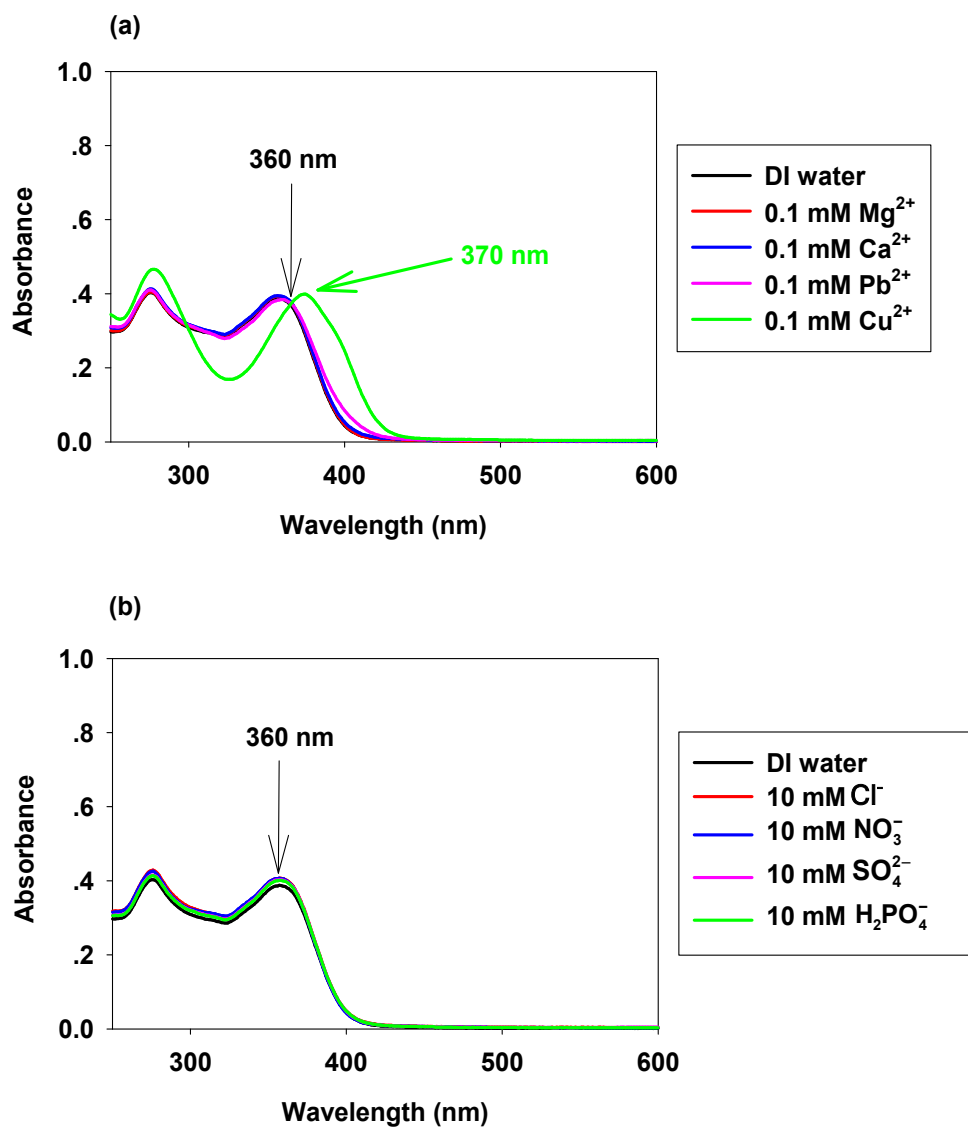


Fig. S2 UV/Vis spectra of tetracycline (10 mg/L) under different solution chemistry conditions: (a) different divalent metal cations; (b) different inorganic anions.

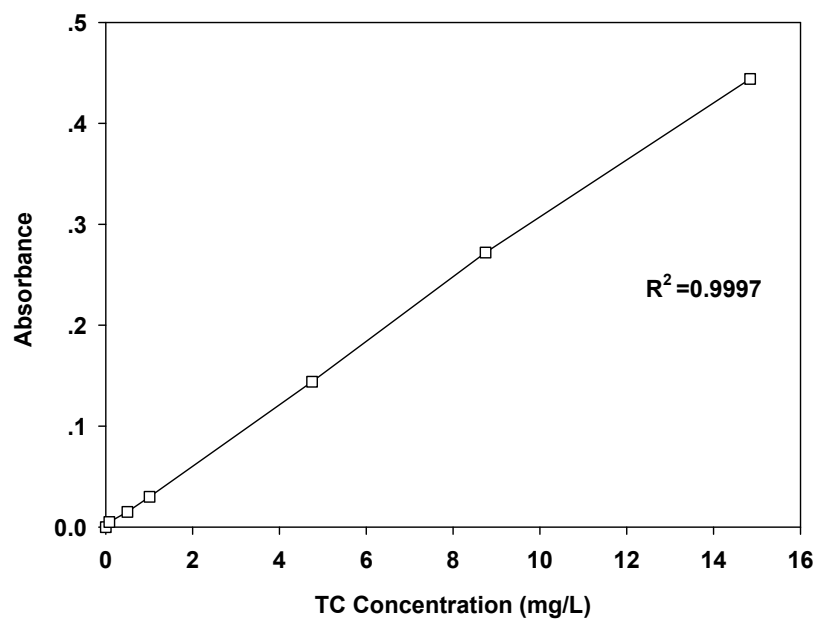


Fig. S3 Calibration curve as absorbance at the wavelength of 360 nm vs. concentration of tetracycline in suspension.

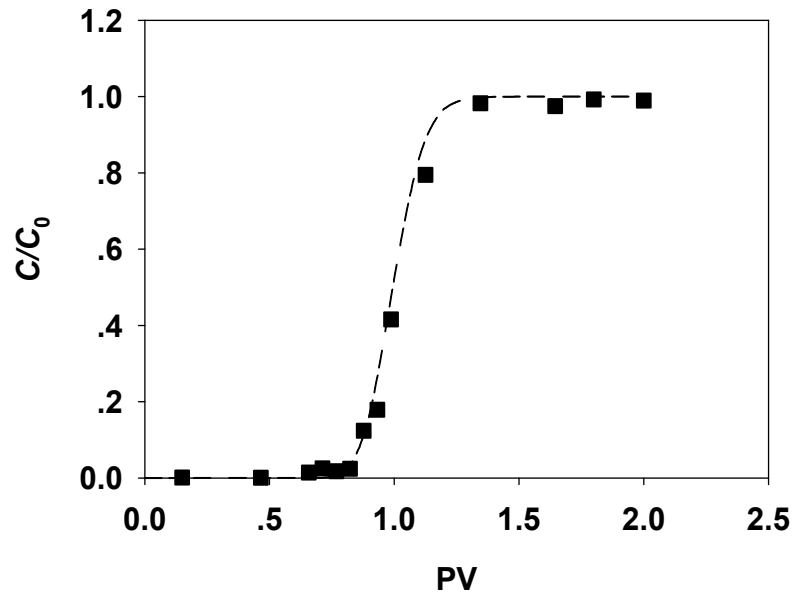


Fig. S4 Representative breakthrough curve of conservative tracer (Br⁻). The line was plotted by fitting the breakthrough data with the one-dimensional steady-state advection–dispersion equation.

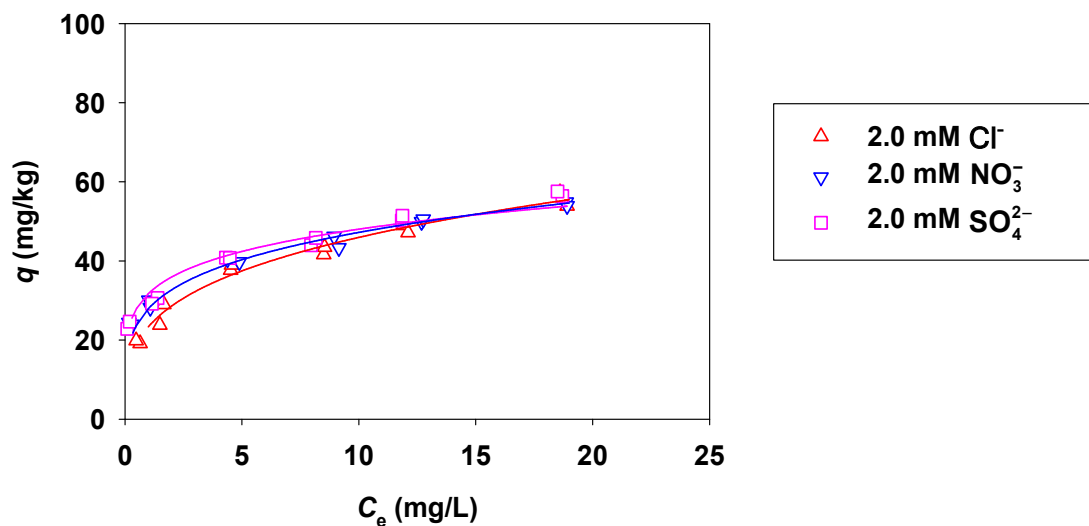


Fig. S5 Sorption isotherms of tetracycline onto quartz sand at 2 mM inorganic anions (Ca^{2+} is the counterion in the background solution). Symbols are experimental data and lines are plotted by fitting the data with Freundlich sorption isotherm.

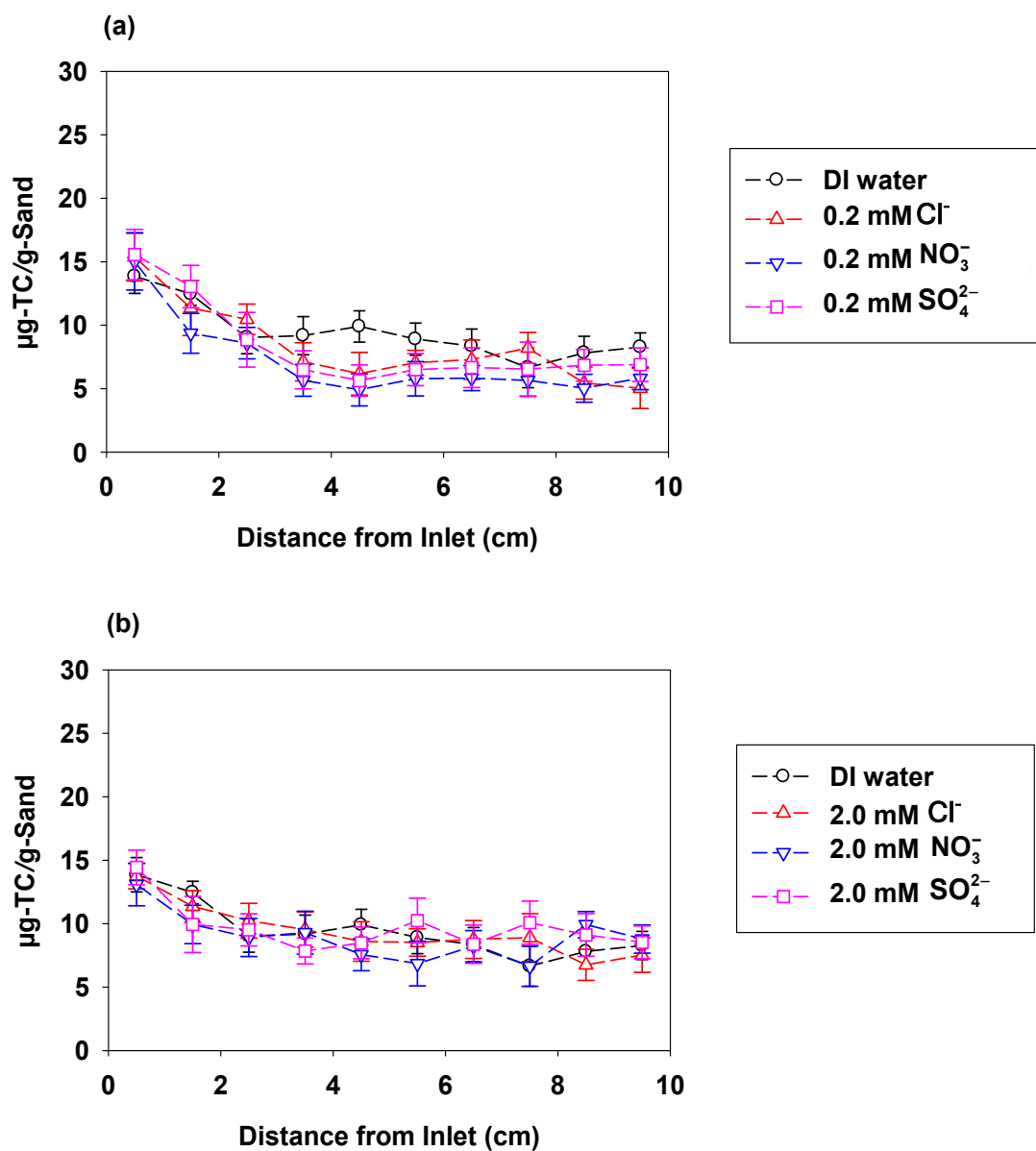


Fig. S6 Retained profiles of tetracycline for transport under different inorganic anions when Ca^{2+} is the counterion in the background solution: (a) 0.2 mM inorganic anions (columns 3, 10–11); (b) 2.0 mM inorganic anions (columns 12–14).

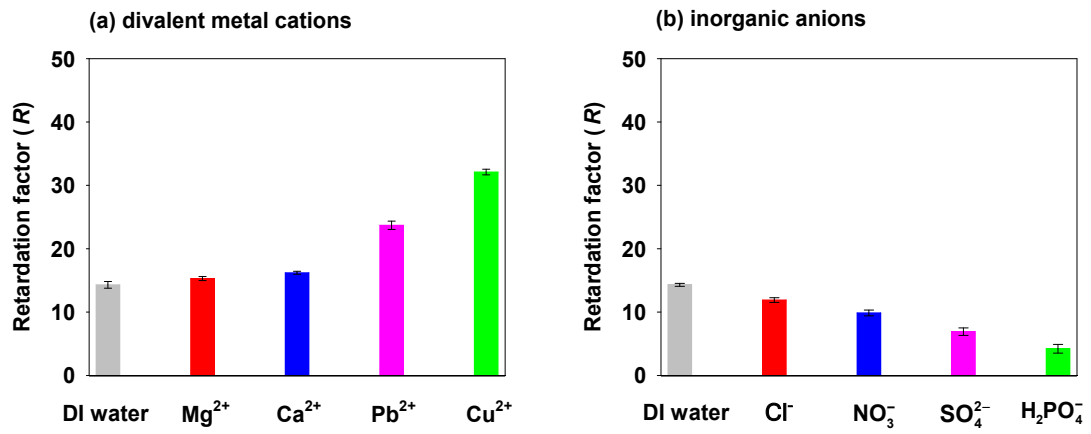


Fig. S7 Retardation factor (*R*) of tetracycline in sand columns under (a) different divalent metal cations and (b) different inorganic anions.

References

- S1. J. Fang, M. Wang, B. Shen, L. Zhang and D. Lin, Distinguishable co-transport mechanisms of phenanthrene and oxytetracycline with oxidized multiwalled carbon nanotubes through saturated soil and sediment columns: vehicle and competition effects. *Water Res.* 2017, **108**, 271–279.
- S2. P. H. Chang, Z. Li, J. S. Jean, W. T. Jiang, C. J. Wang and K. H. Lin, Adsorption of tetracycline on 2:1 layered non-swelling clay mineral illite. *Appl. Clay Sci.* 2012, **67–68**, 158–163.
- S3. J. Li, K. Zhang and H. Zhang, 2018. Adsorption of antibiotics on microplastics. *Environ. Pollut.* 2018, **237**, 460–467.
- S5. M. Y. Kiriukhin and K. D. Collins, Dynamic hydration numbers for biologically important ions. *Biophys. Chem.* 2002, **99**, 155–168.
- S6. B. Tansel, Significance of thermodynamic and physical characteristics on permeation of ions during membrane separation: hydrated radius, hydration free energy and viscous effects, *Sep. Purif. Technol.* 2012, **86**, 119–126.